*Journal of Metals, Materials and Minerals, 36(1), e2412, 2026*

# Synthesis and photoluminescence properties of graphene quantum dots prepared via carbonization under pressure reduction

Sutthipoj WONGRERKDEE[1], and Pichitchai PIMPANG[2,*]

[1] *Department of Physical and Material Sciences, Faculty of Liberal Arts and Science, Kasetsart University Kamphaeng Saen Campus, Nakhon Pathom 73140, Thailand*

[2] *Faculty of Science and Technology, Pibulsongkram Rajabhat University, Phitsanulok 65000, Thailand*

***Corresponding author e-mail**: p.pimpang@psru.ac.th

**Received date:**
26 May 2025
**Revised date:**
21 August 2025
**Accepted date:**
5 November 2025

**Keywords:**
Graphene quantum dots;
Carbonization;
Reduced pressure;
Photoluminescence;
Citric acid precursor

**Abstract**

This study reports the synthesis of graphene quantum dots (GQDs) via a bottom-up carbonization approach using citric acid as a precursor under various reduced pressure conditions. The carbonization process was carried out at 250°C in an ethanol medium, with atmospheric pressures ranging from normal to 20 inHg below atmospheric pressure. The effects of pressure reduction on the size and optical properties of GQDs were systematically investigated. Dynamic light scattering (DLS), UV–Vis spectroscopy, and fluorescence spectroscopy revealed that pressure reduction during synthesis decreased GQDs size and induced a blue-shift in both absorption and emission spectra. The optical bandgap of GQDs was tunable by varying the synthesis pressure, and strong blue fluorescence was observed under UV excitation. FT-IR analysis confirmed the formation of functional groups on the GQD surface, while the absence of epoxy-related bands indicated complete carbonization of the precursor. These findings demonstrate that pressure-controlled carbonization offers an effective method for tailoring the structural and photoluminescent properties of GQDs, enabling their application in optoelectronic and sensing devices.

## 1. Introduction

Graphene quantum dots (GQDs) have emerged as zero-dimensional carbon-based nanomaterials that combine the exceptional properties of graphene with the size-dependent characteristics of quantum dots. GQDs are typically less than 10 nm in size and consist of a few layers of graphene sheets with abundant oxygen-containing functional groups on their surfaces. These quantum dots possess unique optical and electronic properties due to the quantum confinement effect and edge effects, which are not present in bulk graphene. These properties include tunable photoluminescence, high surface-to-volume ratio, chemical stability, biocompatibility, and excellent solubility in various solvents. Such features make GQDs highly promising for a wide range of applications including optoelectronics, biosensing, bioimaging, drug delivery, and energy-related devices [1,2]. GQDs were developed to address a key limitation of graphene. Although graphene has excellent mechanical, thermal, and electrical properties, it lacks a bandgap, which is essential for semiconductor functionality. However, when graphene is reduced to the quantum dot scale, the previously absent bandgap begins to emerge. The bandgap of GQDs can be tuned by controlling their size, shape, number of layers, and surface functionalization. Quantum confinement induces broad-spectrum photoluminescence, enabling applications in LEDs, solar cells, and fluorescent probes [3]. Furthermore, GQDs can be easily functionalized with biomolecules, which enhances their selectivity and effectiveness in biosensing platform. In environmental applications, GQDs have been employed as photocatalysts and sensors for detecting heavy metal ions, organic pollutants, and pH changes [4-8]. In energy storage and conversion, they have been used to improve the performance of supercapacitors, lithium-ion batteries, and fuel cells [9].

Synthesis of GQDs is typically categorized into two main strategies: top-down and bottom-up approaches. The top-down approach involves breaking down bulk carbon materials such as graphite, graphene oxide (GO), carbon nanotubes (CNTs), and carbon fibers into nanoscale quantum dots. Methods used in this approach include chemical oxidation, electrochemical exfoliation, hydrothermal and solvothermal cutting, and ultrasonication [10,11]. In contrast, bottom-up approaches build GQDs from small organic molecules through carbonization, pyrolysis, or molecular self-assembly [6,12-15]. In these methods, suitable organic precursors can be thermally decomposed to produce GQDs with high photoluminescence quantum yields. Among bottom-up techniques, carbonization method is particularly attractive because it enables a one-step synthesis of GQDs without the need for toxic reagents or complex equipment. Moreover, the use of low-cost, renewable precursors such as citric acid and glucose aligns well with green chemistry principles. Carbonization involves the thermal decomposition of organic precursors to form carbon-rich nanostructures, with their properties finely tunable through control of parameters such as temperature, time, atmosphere, and precursor concentration. [14,16]. Accordingly, optimizing carbonization conditions and exploring novel precursors will further enhance the capabilities and commercial potential of GQDs.

*DOI:10.55713/jmmm.v36i1.2412*

This study investigates the effect of pressure reduction on the size and optical properties of graphene quantum dots (GQDs). GQDs were synthesized by carbonizing citric acid at 250°C. A 0.1 M solution of citric acid was prepared by dissolving citric acid monohydrate powder in ethanol, which has been reported as a promising solvent for citric acid [17]. Optimized carbonization conditions were explored under various atmospheric pressures, including normal pressure and reduced pressures of 5 inHg, 10 inHg, 15 inHg, and 20 inHg below atmospheric pressure, all controlled using a gauge meter. The microstructure of GQDs was analyzed using dynamic light scattering (DLS) and Fourier-transform infrared (FT-IR) spectroscopy. Optical properties of the GQDs were characterized by UV–Vis spectroscopy and fluorescence spectroscopy.

## 2. Experimental detail

To investigate the effect of pressure reduction on the size and optical properties of graphene quantum dots (GQDs), citric acid precursor was subjected to carbonization under various atmospheric pressures, including normal pressure and reduced pressures of 5 inHg, 10 inHg, 15 inHg, and 20 inHg below atmospheric level. A vacuum pump was used to reduce the pressure, which was monitored and controlled using a pressure control valve, as shown in Figure 1. To synthesize GQDs, a precursor solution was firstly prepared by dissolving 2.1120 g of citric acid monohydrate (99.5%, Loba Chemie; MW 210.14 g·mol$^{-1}$) in 100 mL of ethanol (99.5%, Merck) to obtain a 0.1 M solution, stirred at room temperature until clear and colorless [14]. Next, a 500 mL Pyrex erlenmeyer flask was closed with a rubber stopper, preheated to 250°C on a hot plate stirrer (IKA C-MAG HS7), and the pressure was subsequently reduced using a vacuum pump. Following this, 100 mL of the precursor solution was added dropwise into the heated flask using a peristaltic pump at a flow rate of 3 mL·min$^{-1}$ to maintain a consistent reaction temperature. Upon heating, ethanol evaporated and the citric acid precursor transitioned from a colorless solution to a molten yellow state. The visibly molten yellow product and strong blue fluorescence under 365 nm excitation indicated GQDs formation [14]. To preserve the product, it was cooled to room temperature and ethanol was added to restore the original volume.

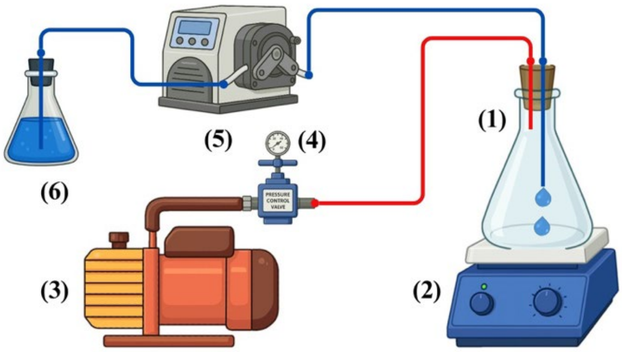

**Figure 1**. Experimental setup for GQDs synthesis via carbonization under reduced pressure, including: (1) an Erlenmeyer flask closed with a rubber stopper, (2) a hot plate stirrer, (3) a vacuum pump, (4) a pressure control valve, (5) a peristaltic pump, and (6) an Erlenmeyer flask containing a citric acid solution, also closed with a rubber stopper.

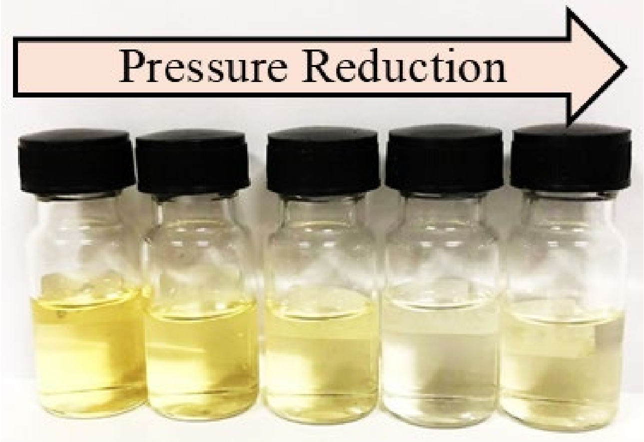

**Figure 2**. Photographs of GQDs synthesized via the carbonization process under different pressures, including normal pressure and reduced pressures of 5 inHg, 10 inHg, 15 inHg, and 20 inHg below atmospheric level.

GQDs characterization of size and surface functional groups were characterized using dynamic light scattering (DLS, Malvern Zetasizer Nano S) and FT-IR spectroscopy (Thermo scientific Nicolet$^{TM}$ iS), while optical properties were analyzed by UV–Vis (Shimadzu UV-2450) and fluorescence spectroscopy (Shimadzu RF-6000). DLS size distributions were measured from 0.3 nm to 10 µm. FT-IR spectra were collected in the range of 500 cm$^{-1}$ to 4000 cm$^{-1}$, UV–Vis absorption spectra were obtained in the range of 200 nm to 700 nm. Excitation–emission contour maps were obtained using excitation wavelengths between 300 nm to 400 nm. Fluorescence spectra were performed in the range of 400 nm to 700 nm with excitation wavelengths of 365 nm.

## 3. Results and discussion

Figure 2 presents photographs of graphene quantum dots (GQDs) dispersed in pure ethanol, synthesized through the carbonization process under varying pressure conditions—specifically at normal atmospheric pressure and under reduced pressures of 5 inHg, 10 inHg, 15 inHg, and 20 inHg below atmospheric level. A noticeable shift in the solution color was observed, transitioning from a vivid yellow at atmospheric pressure to a progressively more translucent yellow as the pressure decreased. Accordingly, the optical absorption of synthesized GQDs were investigated.

Optical absorption of GQDs were evaluated using UV-vis absorbance spectra (Figure 3). GQDs showed strong UV absorption, with the edge shifting from 330 nm to 308 nm under reduced pressure. The UV absorption at near 320 nm corresponds to n–π* transitions of C=C bonds. The observed blue-shift, attributed to reduced GQDs size, aligns with previous reports [14,18]. Additionally, GQDs exhibited visible absorption around 380 nm to 390 nm, and their absorption decreased with decreasing atmospheric pressure. The visible light absorption of GQDs is strongly influenced by the presence of partially conjugated π-electron systems within their layered structures. These systems arise from small sp$^2$ domains and structural imperfections, leading to π–π* transitions typically observed around 380 nm to 390 nm. A lower degree of π-conjugation may result from these structural changes [19,20]. Interestingly, under lower atmosphere pressure level, a noticeable reduction in the intensity of visible light absorption was observed. This suggests that lower synthesis pressures may lead to less efficient carbonization or increased precursor evaporation under reduced pressure. The correlation between visible absorption and conjugated π-electron networks is consistent with previous studies [19,20], further supporting the role of synthesis conditions in tuning the optical properties of GQDs.

The optical absorption edge of our GQDs shifted from 330 nm to 308 nm under reduced pressure, corresponding to an increase in the estimated optical bandgap from approximately 3.76 eV to 4.03 eV. These values are consistent with previous reports; for example, Ahirwar *et al.* [21] observed absorption features at 253 nm to 279 nm with a shoulder at 325 nm to 370 nm, and reported optical bandgaps in the range of 3.4 eV to 3.8 eV, which are in close agreement with our results.

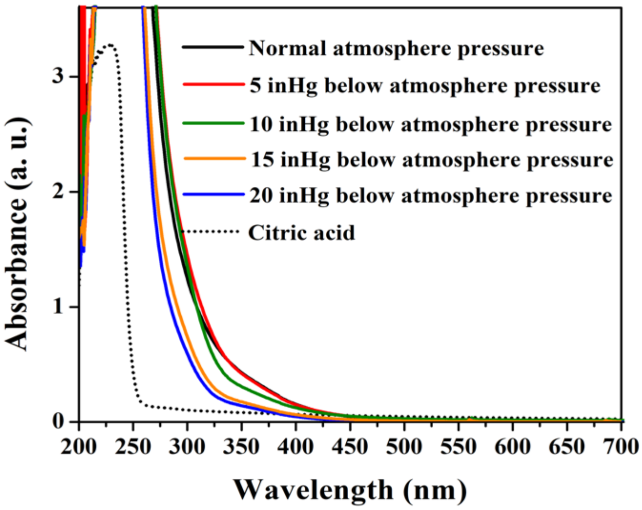

**Figure 3**. UV-vis absorbance spectra of GQDs synthesized via the carbonization process under different pressures, including normal pressure and reduced pressures of 5 inHg, 10 inHg, 15 inHg, and 20 inHg below atmospheric level.

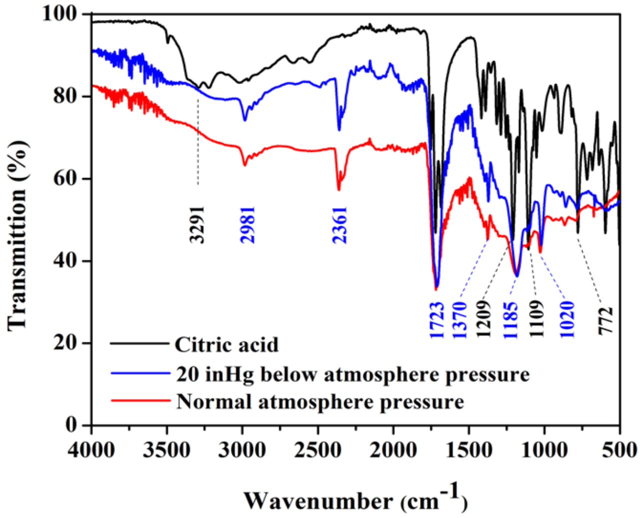

**Figure 4**. Representative FT-IR spectra of citric acid and GQDs synthesized via the carbonization process under normal pressure and reduced pressures of 20 inHg below atmospheric level.

Representative FT-IR spectra of citric acid and GQDs synthesized via carbonization under normal atmospheric pressure and under a reduced pressure of 20 inHg below atmospheric level are shown in Figure 4. The FT-IR spectra of GQDs synthesized under 20 inHg below atmospheric pressure was representative of all reduced-pressure conditions, as the spectra remained essentially unchanged. It was found that citric acid exhibited a broad O–H stretching band (R–C(O)–OH) at around 3291 $cm^{-1}$, a C=O stretching band (C(O)–OH) at 1723 $cm^{-1}$, C–OH stretching at 1109 $cm^{-1}$, and $CH_2$ rocking at 772 $cm^{-1}$. These bands are attributed to the vibrational modes of the citric acid molecule [14]. In contrast, the FT-IR spectrum of GQDs showed no detectable O–H stretching band, implying that the citric acid monohydrate decomposed and carbonized completely. Additionally, the GQDs exhibited C–H stretching at 2981 $cm^{-1}$, C=O stretching (C(O)–OH) at 1723 $cm^{-1}$ [16], C–OH stretching at 1185 $cm^{-1}$, and C–O stretching at 1020 $cm^{-1}$, indicating hydroxyl and carboxyl groups on the functionalized GQD surface [19]. Notably, no C–O–C stretching band was detected around 1050 $cm^{-1}$ to 1250 $cm^{-1}$, which typically indicates the presence of epoxy or ether groups commonly found in oxidized carbon materials [22]. While FT-IR spectra already provide clear evidence of successful carbonization and the presence of hydroxyl and carboxyl functional groups on the GQD surface, we acknowledge the limitation of relying solely on FT-IR for assessing surface functionalities and carbonization degree. Complementary techniques such as X-ray photoelectron spectroscopy (XPS) and Raman spectroscopy would provide more detailed insights into the bonding environment and $sp^2$ domain formation, as well as independent confirmation of the absence of epoxy-related bands. Although these measurements are not included in the present study, the combination of FT-IR results with the observed pressure-dependent optical behavior strongly supports the interpretation that the GQDs are well carbonized and possess functionalized $sp^2$ domains. Future work will incorporate XPS and Raman analyses to further validate these findings.

Figure 5 presents the DLS size distributions of GQDs synthesized by carbonization under different reduced pressure conditions. The distributions, obtained from ten repeated measurements, indicate a decrease in the average GQD size from 0.73 nm to 0.67 nm as the pressure is reduced. It should be noted that the sub-1 nm average values represent hydrodynamic diameters and thus reflect contributions from both lateral and vertical dimensions of the GQD platelets. Although DLS was employed to estimate particle size, it is well recognized that the technique has limited reliability for ultrasmall nanoparticles and cannot provide accurate absolute values below 1 nm. Therefore, in this study the DLS data were used primarily to monitor relative size trends among samples synthesized under different pressure conditions rather than to report precise dimensions.

Fluorescence properties of GQDs were characterized using fluorescence spectroscopy. Figure 6 shows excitation–emission contour maps of GQDs synthesized via carbonization at normal pressure and under reduced pressures of 5 inHg, 10 inHg, 15 inHg, and 20 inHg below atmospheric level. It was found that the maximum excitation wavelength decreased from 375 nm to 350 nm with reduced pressure. Notably, the maximum emission wavelength shifted from 462 to 450 nm as pressure decreased.

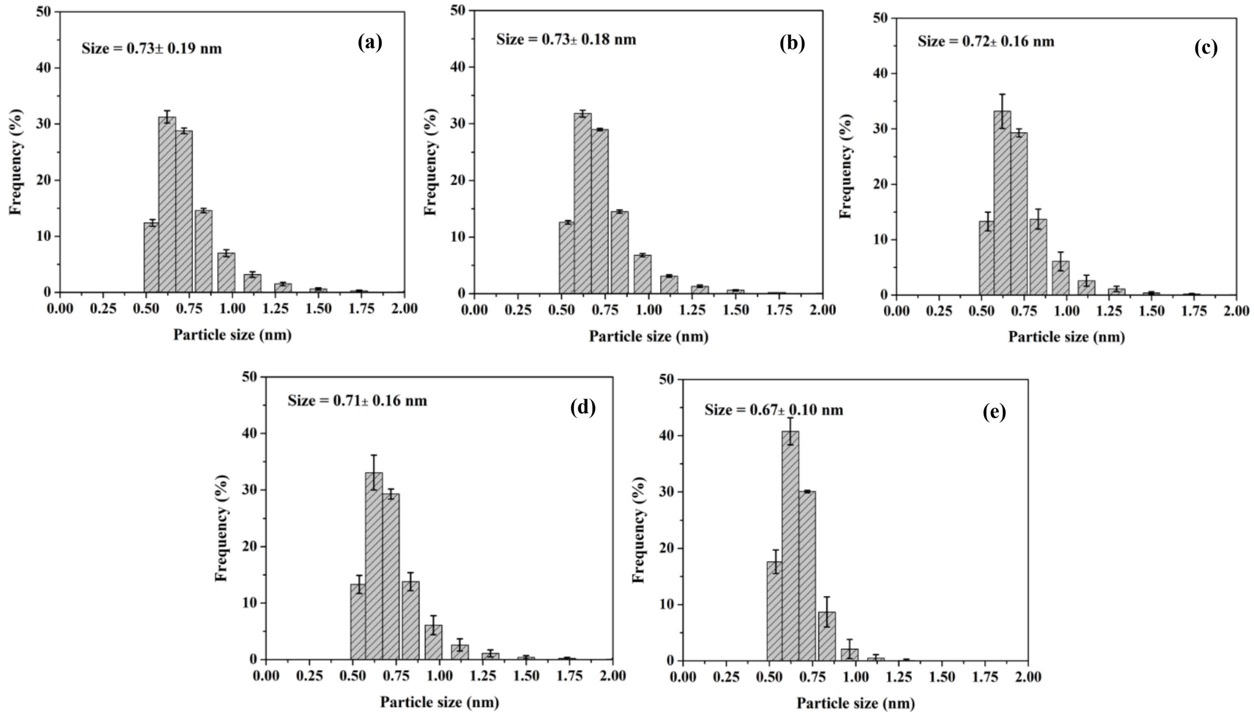

**Figure 5**. DLS size distributions of GQDs synthesized via the carbonization process under different pressures, including normal pressure (a) and reduced pressures of 5 inHg, 10 inHg, 15 inHg, and 20 inHg below atmospheric level, shown in (b)-(e), respectively.

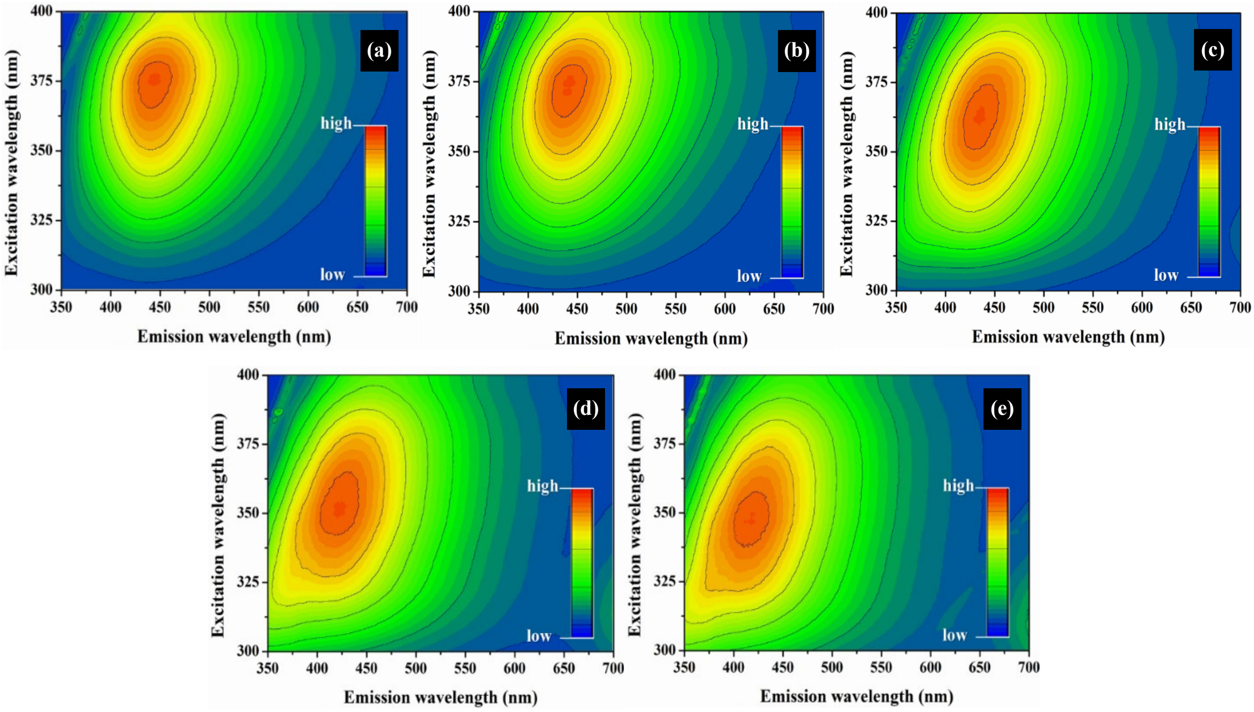

**Figure 6**. Excitation–emission contour maps of GQDs synthesized via carbonization at normal pressure (A) and under reduced pressures of 5, 10, 15, and 20 inHg below atmospheric level (B–E).

Accordingly, the fluorescence spectra, shown in Figure 7, were observed in the visible region. The inset displays the strong blue fluorescence observed under 365 nm UV irradiation. To gain deeper insight into GQD emission, fluorescence analysis revealed strong blue emission under 365 nm excitation [12,14,23–25]. It was found that the peak fluorescence wavelength decreased from 456 nm to 445 nm with reduced pressure. This blue-shift in emission, attributed to reduced GQDs size, aligns with previous reports [14,18,26]. Accordingly, the optical properties confirm a non-zero bandgap and tunable fluorescence controllable by reduced pressure conditions. Notably, quantum yield (QY) measurements would provide a valuable quantitative benchmark to compare our GQDs with other synthesis methods and to further highlight their potential in optoelectronic applications. However, QY measurements were not performed in this study due to instrument limitations.

Importantly, the systematic blue-shifts observed in the UV–vis absorption edge and the photoluminescence emission peak are consistent with the DLS-derived size trends. This strong agreement between optical properties and DLS measurements provides indirect but compelling evidence that reduced carbonization pressure promotes the formation of smaller GQDs.

The pressure-dependent optical behavior observed in this study can be explained by nucleation and growth theory under non-equilibrium conditions. When the synthesis is carried out under reduced pressure, solvent evaporation is accelerated, which rapidly increases supersaturation and induces burst nucleation. As a result, numerous but smaller $sp^2$ domains are formed, while their subsequent growth is limited, smaller GQDs and a blue-shift in both absorption and emission spectra. This interpretation is supported by previous findings. Wang *et al.* [27] showed that reduced pressure alters nucleation and growth kinetics during solvent evaporation crystallization, while de Bruijn *et al.* [28] demonstrated theoretically that faster evaporation reduces induction time and enhances nucleation flux under non-stationary conditions. Similarly, studies on low-pressure CVD growth of graphene have reported that decreasing background pressure increases nucleation density and decreases domain size. In addition, Pimpang *et al.* [14] investigated the effect of precursor concentration on GQD formation and explained size reduction and optical blue-shift in terms of nucleation and growth, using Classical Nucleation Theory (CNT). According to CNT, the critical nucleus size ($r_{critical}$) and nucleation barrier decrease ($\Delta G_{critical}$) as supersaturation (S) increase. Specifically, $r_{critical}$ α 1/In S and $\Delta G_{critical}$ α 1/(In S)$^2$. This theoretical prediction is in good agreement with our experimental observations under reduced pressure. Together, these studies provide a coherent framework supporting that reduced pressure enhances supersaturation, modifies carbonization kinetics, and alters nucleation pathways of $sp^2$ domains, thereby controlling the size and optical properties of GQDs.

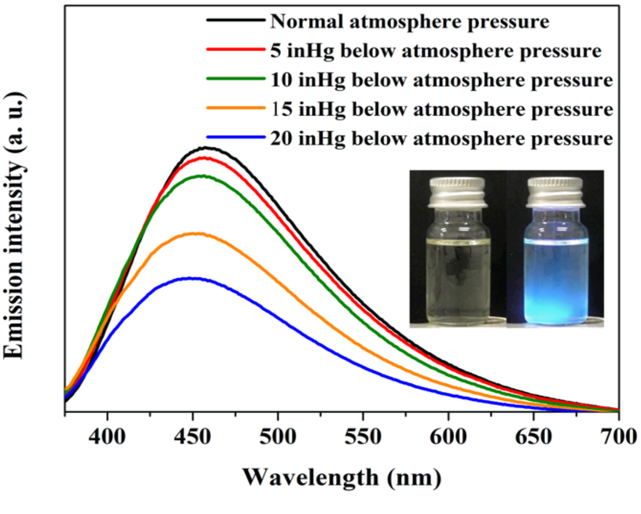

**Figure 7**. Fluorescence spectra of GQDs synthesized via the carbonization process under different pressures, including normal pressure and reduced pressures of 5, 10, 15, and 20 inHg below atmospheric level. Fluorescence spectra were recorded at an excitation wavelength of 365 nm.

## 4. Conclusions

Graphene quantum dots (GQDs) were successfully synthesized via a carbonization method using citric acid as a precursor under various reduced pressure conditions. The study demonstrated that pressure reduction during synthesis significantly influences the size and optical properties of the resulting GQDs. As the synthesis pressure decreased, the average particle size reduced and both UV–Vis absorption and fluorescence spectra exhibited a notable blue-shift, indicating the tunability of optical properties through pressure control. FT-IR analysis confirmed the effective carbonization of citric acid and the presence of surface functional groups such as carboxyl and hydroxyl. The findings highlight that carbonization under reduced pressure provides a simple and efficient route to produce GQDs with enhanced and controllable photoluminescent properties, suggesting strong potential for applications in optoelectronic devices, sensors, and related nanotechnology fields. In particular, pressure-controlled GQDs may be applied in blue/UV light-emitting diodes, photodetectors, bioimaging probes, and fluorescence-based sensors for heavy metal or pesticide detection.

## Acknowledgments

Financial support from Pibulsongkram Rajabhat University (Grant No. RDI-1-68-48) is acknowledged. The authors acknowledge the Science Center Faculty of Science and Technology, Pibulsongkram Rajabhat University for providing measurement instruments. The authors also wish to thank Department of Physical and Material Sciences, Faculty of Liberal Arts and Science, Kasetsart University Kamphaeng Saen Campus for providing supporting facilities.

## References

[1] S. Zhu, Y. Song, X. Zhao, J. Shao, J. Zhang, and B. Yang, “The photoluminescence mechanism in carbon dots (graphene quantum dots, carbon nanodots, and polymer dots): current state and future perspective,” *Nano Research,* vol. 8, no. 2, pp. 355–381, 2015.

[2] H. Sun, L. Wu, W. Wei, and X. Qu, “Recent advances in graphene quantum dots for sensing,” *Materials Today*, vol. 16, no. 11, pp. 433–442, 2013.

[3] S. Bak, D. Kim, and H. Lee, “Graphene quantum dots and their possible energy applications: A review,” *Current Applied Physics*, vol. 16, no. 9, 1192–1201, 2016.

[4] T. F. Yeh, C. Y. Teng, S. J. Chen, and H. Teng, “Nitrogen-doped graphene oxide quantum dots as photocatalysts for overall water-splitting under visible light illumination,” *Advanced Materials*, vol. 26, no. 20, pp. 3297–3303, 2014.

[5] H. Liu, H. Wang, Y. Qian, J. Zhuang, L. Hu, Q. Chen, and S. Zhou, “Nitrogen-doped graphene quantum dots as metal-free photocatalysts for near-infrared enhanced reduction of 4-nitrophenol,” *ACS Applied Nano Materials*, vol. 2, no. 11, pp. 7043–7050, 2019.

[6] S. Wongrerkdee, and P. Pimpang, “Fluorescence quenching probe based on graphene quantum dots for detection of copper

ion in water," *Integrated Ferroelectrics*, vol. 222, no. 1, pp. 56–68, 2022.

[7] M. P. Croxall, R. T. Lawrence, R. G. Biswas, R. Soong, A. J. Simpson, and M. C. Goh, "Improved photocatalytic performance of $TiO_2$–nitrogen-doped graphene quantum dot composites mediated by heterogeneous interactions," *The Journal of Physical Chemistry Letters*, vol. 15, no. 13, pp. 3653–3657, 2024.

[8] C. Raktham, S. Wongrerkdee, and P. Pimpang, "Utilizing nitrogen-doped graphene quantum dots to modify ZnO for enhanced photocatalytic activity in commercial insecticide degradation," *PSRU Journal of Science and Technology*, vol. 9, no. 3, pp. 82–93, 2024

[9] Z. Zhang, J. Zhang, N. Chen, and L. Qu, "Graphene quantum dots: an emerging material for energy-related applications and beyond," *Energy & Environmental Science*, vol. 5, no. 10, pp. 8869–8890, 2012.

[10] D. Pan, J. Zhang, Z. Li, and M. Wu, "Hydrothermal route for cutting graphene sheets into blue-luminescent graphene quantum dots," *Advanced Materials*, vol. 22, no. 6, pp. 734–738, 2010.

[11] Y. Li, Y. Hu, Y. Zhao, G. Shi, L. Deng, Y. Hou, and L. Qu, "An electrochemical avenue to green-luminescent graphene quantum dots as potential electron-acceptors for photovoltaics," *Advanced Materials*, vol. 23, no. 6, pp. 776–780, 2010.

[12] Y. Dong, J. Shao, C. Chen, H. Li, R. Wang, Y. Chi, X. Lin, and G. Chen, "Blue luminescent graphene quantum dots and graphene oxide prepared by tuning the carbonization degree of citric acid," *Carbon*, vol. 50, no. 12, pp. 4738–4743, 2012.

[13] L. Tang, R. Ji, X. Li, G. Bai, C. P. Liu, J. Hao, J. Lin, H. Jiang, K. S. Teng, Z. Yang, and S. P. Lau, "Deep ultraviolet to near-infrared emission and photoresponse in layered N-doped graphene quantum dots," *ACS Nano*, vol. 8, no. 6, pp. 6312–6320, 2014.

[14] P. Pimpang, R. Sumang, and S. Choopun, "Effect of concentration of citric acid on size and optical properties of fluorescence graphene quantum dots prepared by tuning carbonization degree," *Chiang Mai Journal of Science*, vol. 45, no. 5, pp. 2005–2014, 2018.

[15] S. Wongrerkdee, and P. Pimpang, "Ultraviolet-shielding and water resistance properties of graphene quantum dots/polyvinyl alcohol composite-based film," *Journal of Metals, Materials and Minerals*, vol. 30, no. 4, pp. 90–96, 2020.

[16] J. P. Naik, P. Sutradhar, and M. Saha, "Molecular scale rapid synthesis of graphene quantum dots (GQDs)," *Journal of Nanostructure in Chemistry*, vol. 7, pp. 85–89, 2017.

[17] M. L. N. Oliveira, R. A. Malagoni, and M. R. Franco, "Solubility of citric acid in water, ethanol, n-propanol and in mixtures of ethanol+water," *Fluid Phase Equilibria*, vol. 352, pp. 110–113, 2013.

[18] S. Bak, D. Kim, and H. Lee, "Graphene quantum dots and their possible energy applications: A review," *Current Applied Physics*, vol. 16, no. 9, pp. 1192–1201, 2016.

[19] L. Tang, R. Ji, X. Li, G. Bai, C. P. Liu, J. Hao, J. Lin, H. Jiang, K. Seng, Z. Yang, and S. P. Lau, "Deep ultraviolet to near-infrared emission and photoresponse in layered N-doped graphene quantum dots," *ACS Nano*, vol. 8, no. 6, pp. 6312–6320, 2014.

[20] L. Song, J. Shi, J. Lu, and C. Lu, "Structure observation of graphene quantum dots by single-layered formation in layered confinement space," *Chemical Science*, vol. 6, no. 8, pp. 4846–4850, 2015.

[21] S. Ahirwar, S. Mallick, and D. Bahadur, "Electrochemical method to prepare graphene quantum dots and graphene oxide quantum dots," *ACS Omega*, vol. 2, no. 11, pp. 8343–8353, 2017.

[22] D. R. Dreyer, S. Park, C. W. Bielawski, and R. S. Ruoff, "The chemistry of graphene oxide," *Chemical Society Reviews*, vol. 39, no. 1, pp. 228–240, 2010.

[23] J.-J. Liu, Z.-T. Chen, D.-S. Tang, Y.-B. Wang, L.-T. Kang, and J.-N. Yao, "Graphene quantum dots-based fluorescent probe for turn-on sensing of ascorbic acid," *Sensors and Actuators B: Chemical*, vol. 212, pp. 214–219, 2015.

[24] F. A. Permatasari, A. H. Aimon, F. Iskandar, T. Ogi, and K. Okuyama, "Role of C–N configurations in the photoluminescence of graphene quantum dots synthesized by a hydrothermal route," *Scientific Reports*, vol. 6, p. 21042, 2016.

[25] L. Wang, W. Li, B. Wu, Z. Li, S. Wang, Y. Liu, D. Pan, and M. Wu, "Facile synthesis of fluorescent graphene quantum dots from coffee grounds for bioimaging and sensing," *Chemical Engineering Journal*, vol. 300, pp. 75–82, 2016.

[26] Y. Li, H. Shu, S. Wang, and J. Wang, "Electronic and optical properties of graphene quantum dots: The role of many-body effects," *The Journal of Physical Chemistry C,* vol. 119, no. 9, pp. 4983–4989, 2015.

[27] H. Wang, G. Liu, G. Su, H. Wei, and L. Dang, "Kinetics of ε-CL-20 during reduced pressure evaporation crystallization," *ACS Omega*, vol. 10, no. 24, pp. 25581–25595, 2025.

[28] R. de Bruijn, J. J. Michels, and P. van der Schoot, "Transient nucleation driven by solvent evaporation," *The Journal of Chemical Physics*, vol. 160, no. 8, p. 084505, 2024.